

New Strategies for New Physics Search with $\Lambda_b \rightarrow \Lambda \nu \bar{\nu}$ Decays

Wolfgang Altmannshofer,^{*} Sri Aditya Gadam,[†] and Kevin Toner[‡]

*Department of Physics, University of California Santa Cruz,
and Santa Cruz Institute for Particle Physics,
1156 High St., Santa Cruz, CA 95064, USA*

We examine the new physics sensitivity of the rare decay $\Lambda_b \rightarrow \Lambda \nu \bar{\nu}$ which can be accessible at future Z -pole machines like FCC-ee and CEPC. We find that the longitudinal polarization of Λ_b baryons produced in Z decays introduces a novel observable, the forward-backward asymmetry A_{FB}^\uparrow in the angle between the outgoing Λ momentum and the Λ_b spin. We provide Standard Model predictions for the $\Lambda_b \rightarrow \Lambda \nu \bar{\nu}$ branching ratio and A_{FB}^\uparrow , and show that future precision measurements of these observables are complementary and probe new physics scales comparable to other $b \rightarrow s \nu \bar{\nu}$ and $b \rightarrow s \ell^+ \ell^-$ processes. We also show that the zero crossing of the forward-backward asymmetry offers a robust test of form factor calculations independent of new physics.

I. INTRODUCTION

Rare b decays are highly suppressed in the Standard Model and therefore exceptionally sensitive to new physics at very high energy scales. They garner much effort and attention from the theoretical and experimental communities alike [1, 2].

Precise experimental measurements and accurate SM predictions are essential to fully harness the potential of rare b decays as probes of new physics. Experimental results from LHCb, ATLAS, and CMS exist for a multitude of rare semi-leptonic B meson decays including $B \rightarrow K \mu^+ \mu^-$, $B \rightarrow K^* \mu^+ \mu^-$ and $B_s \rightarrow \phi \mu^+ \mu^-$. Measured observables include differential branching ratios [3–5], angular distributions [6–15], and lepton flavor universality ratios [16–20]. To maximize the potential of rare decay observables in probing new physics, global fits incorporating all relevant rare b decay data are frequently performed,

^{*} waltmann@ucsc.edu

[†] sgadam@ucsc.edu

[‡] ktoner@ucsc.edu

for recent results see [21–30]. Intriguingly, there are several measured branching ratios and angular observables that do not agree well with SM predictions and that fairly consistently point to new physics. The interpretation of the observed deviations in terms of new physics relies critically on the robust control of hadronic effects in $b \rightarrow s\ell^+\ell^-$ decays, parameterized by local and non-local form factors [31–38].

In this context, the rare decays based on the $b \rightarrow s\nu\bar{\nu}$ transition emerge as an interesting complementary probe of new physics [39–44]. The di-neutrino modes are theoretically cleaner than their charged-lepton counterparts, as they are not affected by the non-local hadronic effects (e.g. the charm loops). All hadronic physics in the exclusive $b \rightarrow s\nu\bar{\nu}$ decays is encapsulated by local form factors. The $b \rightarrow s\nu\bar{\nu}$ modes play a dual role in probing new physics: they test heavy new physics through model-independent four-fermion contact interactions (potentially linked to $b \rightarrow s\ell^+\ell^-$ transitions via $SU(2)_L$ symmetry) and provide a window into light dark sectors, as decays like $b \rightarrow sX$ —where X is a neutral, invisibly decaying, or long-lived light particle—mimic the missing-energy signature of di-neutrino processes.

On the experimental side, BaBar and Belle established upper limits on the $B \rightarrow K\nu\bar{\nu}$ and $B \rightarrow K^*\nu\bar{\nu}$ branching ratios a factor of few above the SM predictions [45–48], while Belle II recently found first evidence for $B^+ \rightarrow K^+\nu\bar{\nu}$ [49]. The measured branching ratio is $\sim 2.7\sigma$ above the SM expectation, which sparked renewed interest in the $b \rightarrow s\nu\bar{\nu}$ decays as probes of new physics [50–70]. Belle II is expected to measure the $B^+ \rightarrow K^+\nu\bar{\nu}$ and $B^0 \rightarrow K^{*0}\nu\bar{\nu}$ branching ratios with $\sim 10\%$ precision [71]. Future e^+e^- machines running on the Z -pole like FCC-ee and CEPC [72–75] have the potential to further improve this precision and have the unique capability to observe the $B_s \rightarrow \phi\nu\bar{\nu}$ and $\Lambda_b \rightarrow \Lambda\nu\bar{\nu}$ decays [76, 77]. Combining the insights from the full range of di-neutrino modes—including pseudoscalar-to-pseudoscalar transitions ($B \rightarrow K\nu\bar{\nu}$), pseudoscalar-to-vector transitions ($B \rightarrow K^*\nu\bar{\nu}$, $B_s \rightarrow \phi\nu\bar{\nu}$), and fermion-to-fermion transitions ($\Lambda_b \rightarrow \Lambda\nu\bar{\nu}$)—offers a powerful approach to probing new physics.

The decays of the Λ_b baryon are particularly interesting, as the Λ_b can be polarized and thus provide novel observables that are not accessible in the meson decays. Here, we will be especially interested in the fact that Λ_b baryons that are produced in Z decays are longitudinally polarized [78–82]. The goal of our work is to provide a comprehensive study of the decay $\Lambda_b \rightarrow \Lambda\nu\bar{\nu}$ of longitudinally polarized Λ_b baryons (see [77, 83–87], for related

work on $\Lambda_b \rightarrow \Lambda\nu\bar{\nu}$ decays). The kinematics of the decay is characterized by the energy of the Λ and the angle between its momentum and the spin of the Λ_b . We find that the corresponding angular decay distribution depends on a novel observable, a forward-backward asymmetry A_{FB}^\uparrow , that is proportional to the longitudinal polarization of the Λ_b . We work out state-of-the-art SM predictions for the integrated branching ratio, $\text{BR}(\Lambda_b \rightarrow \Lambda\nu\bar{\nu})$, and the forward-backward asymmetry, A_{FB}^\uparrow , and explore their sensitivity to new physics, in particular to the new physics' chirality structure. See [88] for similar ideas in the context of the $\Lambda_b \rightarrow \Lambda\gamma$ decay.

The corresponding decays with charged leptons in the final state, $\Lambda_b \rightarrow \Lambda\ell^+\ell^-$, have been observed at LHCb [89, 90] and are extensively discussed in the literature [91–98]. It would be interesting to extend our work, and to study the decays of longitudinally polarized $\Lambda_b \rightarrow \Lambda\ell^+\ell^-$, at future Z -pole machines. Note that in our paper, we focus on the decay $\Lambda_b \rightarrow \Lambda\nu\bar{\nu}$, where Λ refers to the weakly decaying Λ baryon ground state. An analogous analysis could also be performed for the $\Lambda_b \rightarrow \Lambda(1520)\nu\bar{\nu}$ decay or other higher excited Λ baryon states. See [99–102] for the relevant transition form factors, and [103–111] for related work on $\Lambda_b \rightarrow \Lambda(1520)\ell^+\ell^-$ decays.

This paper is organized as follows: In section II, we introduce the effective Hamiltonian that describes the $b \rightarrow s\nu\bar{\nu}$ decay in the SM and in models with heavy new physics and define the relevant $\Lambda_b \rightarrow \Lambda$ form factors. We discuss in detail the uncertainties from the short distance SM contributions and the CKM input. In section III, we present our results for the differential $\Lambda_b \rightarrow \Lambda\nu\bar{\nu}$ branching ratio in the presence of longitudinal Λ_b polarization and introduce the forward-backward asymmetry A_{FB}^\uparrow . We give SM predictions for the branching ratio and the forward-backward asymmetry and discuss qualitatively the impact of new physics on the observables. In section IV we determine the new physics sensitivity of precision measurements of the $\Lambda_b \rightarrow \Lambda\nu\bar{\nu}$ observables. Finally, in section V, we discuss the imprint of the forward-backward asymmetry on the Λ energy distribution in the lab frame. This distribution might provide an alternative method to test new physics with $\Lambda_b \rightarrow \Lambda\nu\bar{\nu}$. We conclude in section VI. Details about our implementation of the $\Lambda_b \rightarrow \Lambda$ form factors are collected in appendix A.

II. EFFECTIVE HAMILTONIAN AND HADRONIC MATRIX ELEMENTS

The effective Hamiltonian that underlies the description of the $\Lambda_b \rightarrow \Lambda \nu \bar{\nu}$ decay is

$$\mathcal{H}_{\text{eff}} = -\frac{4G_F}{\sqrt{2}} \frac{\alpha}{4\pi} V_{ts}^* V_{tb} \left(C_L O_L + C_R O_R \right) + \text{h.c.} , \quad (1)$$

with the four-fermion operators

$$O_L = (\bar{s}\gamma^\mu P_L b)(\bar{\nu}\gamma_\mu(1 - \gamma_5)\nu) , \quad O_R = (\bar{s}\gamma^\mu P_R b)(\bar{\nu}\gamma_\mu(1 - \gamma_5)\nu) . \quad (2)$$

In the SM, the Wilson coefficients are $C_L^{\text{SM}} = -X(x_t)/s_W^2$ where $s_W = \sin \theta_W$ is the sine of the weak mixing angle, and $C_R^{\text{SM}} \simeq 0$. The loop function $X(x_t)$ depends on the ratio of the top quark $\overline{\text{MS}}$ mass and the W mass $x_t = m_t^2(m_t)/m_W^2$. Its most recent determination can be found in [112, 113]. The uncertainties in the W mass and the sine of the weak mixing angle s_W can be neglected when evaluating the SM Wilson coefficient, but the uncertainty in the top mass is not entirely negligible.

To obtain a value for C_L^{SM} , we re-scale the $X(x_t)$ function given in [113] to take into account the latest experimental results on the top mass. We translate the top quark pole mass from cross-section measurements quoted by the PDG, $m_t = (172.5 \pm 0.7) \text{ GeV}$ [114], into the top quark $\overline{\text{MS}}$ mass at 3-loop QCD accuracy using RunDec [115] and find $m_t(m_t) = 162.92 \pm 0.72 \text{ GeV}$. Using $m_W = 80.377 \text{ GeV}$ and $s_W^2 = 0.2314$ [114] we arrive at

$$C_L^{\text{SM}} = -6.322 \pm 0.031 \Big|_{m_t} \pm 0.074 \Big|_{\text{QCD}} \pm 0.009 \Big|_{\text{EW}} , \quad (3)$$

where the three uncertainties are due to the top mass, higher-order QCD corrections, and higher-order EW corrections, respectively. The value of the electromagnetic coupling α that enters the effective Hamiltonian is the running α at the electroweak scale, $\alpha^{-1} \simeq 127.95$ with negligible uncertainty.

We determine the relevant CKM matrix elements that enter the effective Hamiltonian from input given by the PDG. In particular, we use [114]

$$|V_{cb}| = (40.8 \pm 1.4) \times 10^{-3} , \quad |V_{ub}| = (3.82 \pm 0.20) \times 10^{-3} , \quad \gamma = 65.9^\circ \pm 3.5^\circ . \quad (4)$$

The values for $|V_{cb}|$ and $|V_{ub}|$ are conservative averages of determinations using inclusive and exclusive tree-level B decays. For the sine of the Cabibbo angle, we use $\lambda \simeq 0.225$ [114], neglecting its tiny uncertainty. This results in

$$|V_{ts}^* V_{tb}|^2 = \left(1.609 \pm 0.109 \Big|_{V_{cb}} \pm 0.001 \Big|_{V_{ub}} \pm 0.004 \Big|_{\gamma} \right) \times 10^{-3} , \quad (5)$$

with the uncertainty entirely dominated by $|V_{cb}|$.

The hadronic matrix elements relevant for the $\Lambda_b \rightarrow \Lambda \nu \bar{\nu}$ decay can be parameterized by form factors in the following way [94, 98, 116]

$$\begin{aligned} \langle \Lambda | \bar{s} \gamma^\mu b | \Lambda_b \rangle = & \bar{u}_\Lambda \left[f_t^V(q^2) (m_{\Lambda_b} - m_\Lambda) \frac{q^\mu}{q^2} + f_\perp^V(q^2) \left(\gamma^\mu - \frac{2(m_\Lambda P^\mu + m_{\Lambda_b} p^\mu)}{(m_{\Lambda_b} + m_\Lambda)^2 - q^2} \right) \right. \\ & \left. + f_0^V(q^2) \frac{m_{\Lambda_b} + m_\Lambda}{(m_{\Lambda_b} + m_\Lambda)^2 - q^2} \left(P^\mu + p^\mu - (m_{\Lambda_b}^2 - m_\Lambda^2) \frac{q^\mu}{q^2} \right) \right] u_{\Lambda_b} , \quad (6) \end{aligned}$$

$$\begin{aligned} \langle \Lambda | \bar{s} \gamma^\mu \gamma_5 b | \Lambda_b \rangle = & -\bar{u}_\Lambda \gamma_5 \left[f_t^A(q^2) (m_{\Lambda_b} + m_\Lambda) \frac{q^\mu}{q^2} + f_\perp^A(q^2) \left(\gamma^\mu + \frac{2(m_\Lambda P^\mu - m_{\Lambda_b} p^\mu)}{(m_{\Lambda_b} - m_\Lambda)^2 - q^2} \right) \right. \\ & \left. + f_0^A(q^2) \frac{m_{\Lambda_b} - m_\Lambda}{(m_{\Lambda_b} - m_\Lambda)^2 - q^2} \left(P^\mu + p^\mu - (m_{\Lambda_b}^2 - m_\Lambda^2) \frac{q^\mu}{q^2} \right) \right] u_{\Lambda_b} , \quad (7) \end{aligned}$$

where P and p are the momenta of the Λ_b and Λ , respectively, and m_{Λ_b} and m_Λ are their masses. The form factors $f_{t,0,\perp}^{V,A}$ are functions of $q^2 = (P - p)^2$, the di-neutrino invariant mass squared. For our numerical analysis, we use the $\Lambda_b \rightarrow \Lambda$ form factors from [94] (see also [98]). More details are provided in appendix A.

III. DIFFERENTIAL BRANCHING RATIO IN THE SM AND BEYOND

With the effective Hamiltonian introduced in the previous section, we can determine the differential branching ratio of the $\Lambda_b \rightarrow \Lambda \nu \bar{\nu}$ decay. For the decay of a polarized Λ_b , the kinematics of the visible decay products depends on two independent variables. One convenient choice is E_Λ , the energy of the Λ in the Λ_b restframe, and θ_Λ , the angle between the Λ momentum and the spin quantization axis of the Λ_b in its restframe. Alternatively, one may want to use the di-neutrino invariant mass squared q^2 and the angle θ_Λ , with q^2 given in terms of the Λ energy by

$$q^2 = m_{\Lambda_b}^2 + m_\Lambda^2 - 2m_{\Lambda_b} E_\Lambda . \quad (8)$$

We find that the double differential branching ratio has a very simple dependence on $\cos \theta_\Lambda$ that can be written as

$$\frac{d\text{BR}(\Lambda_b \rightarrow \Lambda \nu \bar{\nu})}{dE_\Lambda d \cos \theta_\Lambda} = \frac{d\text{BR}(\Lambda_b \rightarrow \Lambda \nu \bar{\nu})}{dE_\Lambda} \left(\frac{1}{2} + A_{\text{FB}}^\uparrow \cos \theta_\Lambda \right) . \quad (9)$$

The differential branching ratio as a function of the Λ energy is given by

$$\frac{d\text{BR}(\Lambda_b \rightarrow \Lambda \nu \bar{\nu})}{dE_\Lambda} = \tau_{\Lambda_b} \frac{\alpha^2 G_F^2}{32\pi^5} m_{\Lambda_b}^5 |V_{ts}^* V_{tb}|^2 \frac{E_\Lambda^2}{m_{\Lambda_b}^3} \sqrt{1 - \frac{m_\Lambda^2}{E_\Lambda^2}} \times \left(|C_L + C_R|^2 \mathcal{F}_V + |C_L - C_R|^2 \mathcal{F}_A \right), \quad (10)$$

where we summed over all three neutrino flavors, assuming that the Wilson coefficients are neutrino flavor conserving and neutrino flavor universal, as is the case in the SM. The numerical value for the Λ_b lifetime that enters the branching ratio is $\tau_{\Lambda_b} = (0.970 \pm 0.009) \times \tau_{B^0} = (1.473 \pm 0.014) \times 10^{-12} \text{ s}$ [114].

The quantity A_{FB}^\uparrow is a forward-backward asymmetry of the Λ with respect to the spin quantization axis of the Λ_b . We find

$$A_{\text{FB}}^\uparrow = \frac{\mathcal{P}_{\Lambda_b} (|C_R|^2 - |C_L|^2) \mathcal{F}_{VA}}{|C_L + C_R|^2 \mathcal{F}_V + |C_L - C_R|^2 \mathcal{F}_A}. \quad (11)$$

To simplify notation in the above expressions for the branching ratio and the forward-backward asymmetry, we have introduced the following quadratic functions of the $\Lambda_b \rightarrow \Lambda$ form factors

$$\mathcal{F}_V = \left(1 - \frac{m_\Lambda}{E_\Lambda} \right) \left((1 + x_\Lambda)^2 (f_0^V(q^2))^2 + \frac{2q^2}{m_{\Lambda_b}^2} (f_\perp^V(q^2))^2 \right), \quad (12)$$

$$\mathcal{F}_A = \left(1 + \frac{m_\Lambda}{E_\Lambda} \right) \left((1 - x_\Lambda)^2 (f_0^A(q^2))^2 + \frac{2q^2}{m_{\Lambda_b}^2} (f_\perp^A(q^2))^2 \right), \quad (13)$$

$$\mathcal{F}_{VA} = \sqrt{1 - \frac{m_\Lambda^2}{E_\Lambda^2}} \left((1 - x_\Lambda^2) f_0^V(q^2) f_0^A(q^2) - \frac{2q^2}{m_{\Lambda_b}^2} f_\perp^V(q^2) f_\perp^A(q^2) \right). \quad (14)$$

All form factors in the above expressions depend on the di-neutrino invariant mass squared q^2 as introduced already in (8). For later convenience, we have introduced the ratio of Λ mass and Λ_b mass $x_\Lambda = m_\Lambda/m_{\Lambda_b}$.

The quantity \mathcal{P}_{Λ_b} that enters the forward-backward asymmetry is the polarization asymmetry of the Λ_b , i.e. it corresponds to the difference of Λ_b baryons with spin-up and spin-down

$$\mathcal{P}_{\Lambda_b} = \frac{N_{\Lambda_b}^\uparrow - N_{\Lambda_b}^\downarrow}{N_{\Lambda_b}^\uparrow + N_{\Lambda_b}^\downarrow}. \quad (15)$$

The natural choice for the spin quantization axis is the direction of the Λ_b momentum in the lab frame. In that case, \mathcal{P}_{Λ_b} corresponds to the longitudinal polarization fraction of the Λ_b .

On the Z pole, this polarization can be measured using semi-leptonic Λ_b decays [78, 117–119]. Measurements at LEP found

$$\mathcal{P}_{\Lambda_b} = \begin{cases} -0.23_{-0.20-0.07}^{+0.24+0.08}, & \text{ALEPH [80]}, \\ -0.49_{-0.30}^{+0.32} \pm 0.17, & \text{DELPHI [82]}, \\ -0.56_{-0.13}^{+0.20} \pm 0.09, & \text{OPAL [81]}, \end{cases} \quad (16)$$

where the first uncertainty is due to statistics and the second due to systematics. A naive weighted average of the LEP measurements that neglects possible correlations gives

$$\mathcal{P}_{\Lambda_b} = -0.40 \pm 0.14. \quad (17)$$

We expect that a future Z pole machine should be able to measure \mathcal{P}_{Λ_b} with percent level accuracy. In fact, the statistical uncertainty at FCC-ee or CEPC should be negligible, while systematic uncertainties from e.g. the lepton energy and missing energy resolution should be improved significantly compared to LEP.¹

A. Standard Model Predictions

Before discussing the new physics sensitivity of the $\Lambda_b \rightarrow \Lambda \nu \bar{\nu}$ decay, we provide the SM predictions for the branching ratio and the forward-backward asymmetry.

The SM expression for the integrated branching ratio can be found from (10), setting the right-handed Wilson coefficient to zero

$$\text{BR}(\Lambda_b \rightarrow \Lambda \nu \bar{\nu})_{\text{SM}} = \tau_{\Lambda_b} \frac{\alpha^2 G_F^2}{32\pi^5} m_{\Lambda_b}^5 |V_{ts}^* V_{tb}|^2 |C_L^{\text{SM}}|^2 \int_{E_{\Lambda}^{\min}}^{E_{\Lambda}^{\max}} \frac{dE_{\Lambda} E_{\Lambda}^2}{m_{\Lambda_b}^3} \sqrt{1 - \frac{m_{\Lambda}^2}{E_{\Lambda}^2}} (\mathcal{F}_V + \mathcal{F}_A), \quad (18)$$

where \mathcal{F}_V and \mathcal{F}_A were already introduced in eqs. (12) and (13), and the integration boundaries are given by

$$E_{\Lambda}^{\min} = m_{\Lambda}, \quad E_{\Lambda}^{\max} = \frac{m_{\Lambda_b}}{2} (1 + x_{\Lambda}^2). \quad (19)$$

We stress that the branching ratio is independent of the Λ_b polarization \mathcal{P}_{Λ_b} .

Using the numerical input discussed previously, we arrive at the following numerical SM prediction for the integrated branching ratio

$$\text{BR}(\Lambda_b \rightarrow \Lambda \nu \bar{\nu})_{\text{SM}} = (7.71 \pm 1.06) \times 10^{-6}, \quad (20)$$

¹ Note that even in the challenging environment of the LHC, measurements of the (transversal) Λ_b polarization with an uncertainty of few percent have been performed [120, 121]

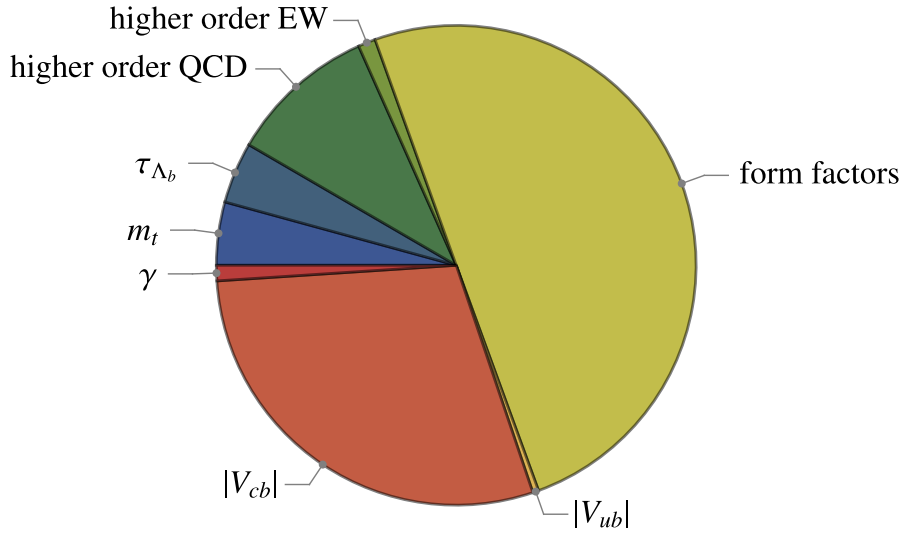


Figure 1. Pie chart that shows the most relevant sources of uncertainty entering the SM prediction of the $\Lambda_b \rightarrow \Lambda \nu \bar{\nu}$ branching ratio.

which has an uncertainty of approximately 14%. In figure 1, we show a pie chart of the various sources of uncertainty that enter our SM prediction. The bulk of the uncertainty is shared by the form factors and the CKM input, with the form factors being dominant. The other sources of uncertainty are subdominant

$$\delta\text{BR}(\Lambda_b \rightarrow \Lambda \nu \bar{\nu})_{\text{SM}} \times 10^6 = \pm 0.90 \Big|_{\text{ff}} \pm 0.53 \Big|_{\text{CKM}} \pm 0.18 \Big|_{\text{QCD}} \pm 0.08 \Big|_{m_t} \pm 0.07 \Big|_{\tau_{\Lambda_b}} \pm 0.02 \Big|_{\text{EW}} = \pm 1.06, \quad (21)$$

where we added all uncertainties in quadrature.

In figure 2, we show the differential branching ratio (10) in the SM as a function of the Λ energy E_Λ (left panel) and the di-neutrino invariant mass squared (right panel). Also these spectra are independent of the Λ_b polarization \mathcal{P}_{Λ_b} . The uncertainty increases for small q^2 or large E_Λ , respectively, as the uncertainties in the form factors increases in that kinematic regime.

The forward-backward asymmetry in the SM is given by

$$(A_{\text{FB}}^\dagger)_{\text{SM}} = \frac{-\mathcal{P}_{\Lambda_b} \mathcal{F}_{VA}}{\mathcal{F}_V + \mathcal{F}_A}. \quad (22)$$

Besides \mathcal{P}_{Λ_b} , the only other source of uncertainty are the form factors contained in the functions \mathcal{F}_V , \mathcal{F}_A , and \mathcal{F}_{VA} in eqs. (12), (13), and (14). In figure 3, we show $(A_{\text{FB}}^\dagger)_{\text{SM}}$ as a

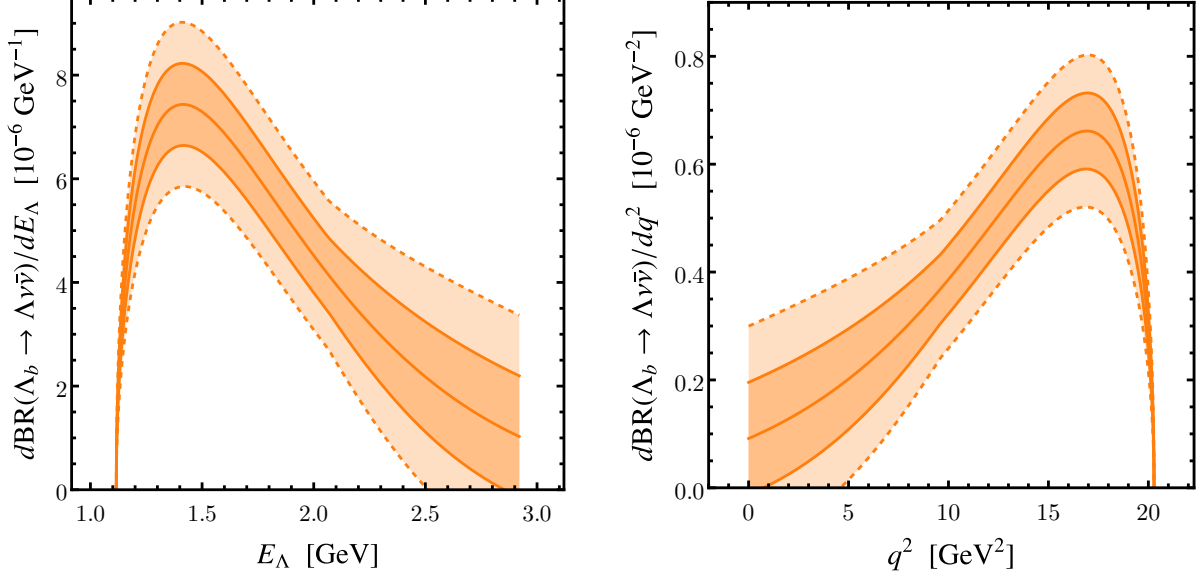


Figure 2. The differential branching ratio of $\Lambda_b \rightarrow \Lambda \nu \bar{\nu}$ in the SM as a function of the Λ energy in the Λ_b rest frame E_Λ (left) and the di-neutrino invariant mass squared q^2 (right). The relevant phase space boundaries of the decay are $m_\Lambda < E_\Lambda < \frac{m_{\Lambda_b}}{2}(1 + m_\Lambda^2/m_{\Lambda_b}^2)$ and $0 < q^2 < (m_{\Lambda_b} - m_\Lambda)^2$. The colored bands correspond to the 1σ and 2σ uncertainties.

function of the Λ energy E_Λ (left panel) and the di-neutrino invariant mass squared (right panel). For concreteness we set the Λ_b polarization to the central value given in eq. (17). The shown uncertainty is from the form factors only. The forward-backward asymmetry vanishes at the kinematic endpoint $E_\Lambda^{\min} = m_\Lambda$, or correspondingly $q_{\max}^2 = (m_{\Lambda_b} - m_\Lambda)^2$. We find that the forward-backward asymmetry has a zero crossing in the SM, which is determined by the relative size of the form factors $f_0^{V,A}$ and $f_\perp^{V,A}$, cf. equation (14), by the implicit relation

$$q^2 = \frac{m_{\Lambda_b}^2}{2} (1 - x_\Lambda^2) \frac{f_0^V(q^2) f_0^A(q^2)}{f_\perp^V(q^2) f_\perp^A(q^2)}. \quad (23)$$

The corresponding numerical zero crossing values for the Λ energy and the di-neutrino invariant mass are

$$(E_\Lambda)_0^{\text{SM}} = (1.80 \pm 0.11) \text{ GeV}, \quad (q^2)_0^{\text{SM}} = (12.6 \pm 1.2) \text{ GeV}^2. \quad (24)$$

The uncertainties in these values are entirely due to the form factors.

Integrating over the whole range of Λ energies we find in the SM

$$\langle A_{\text{FB}}^\uparrow \rangle_{\text{SM}} = -\mathcal{P}_{\Lambda_b} \times \frac{\int_{E_\Lambda^{\min}}^{E_\Lambda^{\max}} dE_\Lambda E_\Lambda^2 \sqrt{1 - \frac{m_\Lambda^2}{E_\Lambda^2}} \mathcal{F}_{VA}}{\int_{E_\Lambda^{\min}}^{E_\Lambda^{\max}} dE_\Lambda E_\Lambda^2 \sqrt{1 - \frac{m_\Lambda^2}{E_\Lambda^2}} (\mathcal{F}_V + \mathcal{F}_A)} = -\mathcal{P}_{\Lambda_b} \times (2.7 \pm 3.4) \times 10^{-2}. \quad (25)$$

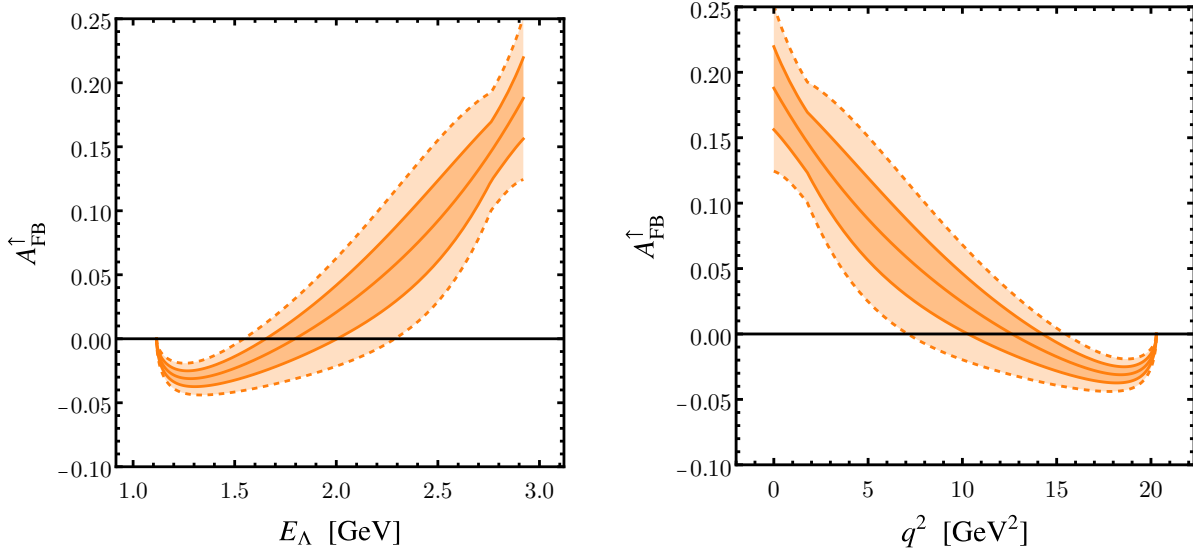


Figure 3. The forward-backward asymmetry in $\Lambda_b \rightarrow \Lambda \nu \bar{\nu}$ in the SM as a function of the Λ energy in the Λ_b rest frame E_Λ (left) and the di-neutrino invariant mass squared q^2 (right). The relevant phase space boundaries of the decay are $m_\Lambda < E_\Lambda < \frac{m_{\Lambda_b}}{2}(1 + m_\Lambda^2/m_{\Lambda_b}^2)$ and $0 < q^2 < (m_{\Lambda_b} - m_\Lambda)^2$. The colored bands correspond to the 1σ and 2σ uncertainties. Only uncertainties due to the form factors are shown. The Λ_b polarization is set to its central experimental value $\mathcal{P}_{\Lambda_b} = -0.40$.

The SM prediction of the integrated asymmetry is fairly small, with the uncertainty entirely due to the form factors. If we instead split the integration region into two parts at the zero crossing of the forward-backward asymmetry, we find

$$\langle A_{\text{FB}}^{\uparrow} \rangle_{\text{SM}}^{\text{low}} = -\mathcal{P}_{\Lambda_b} \times (13.2 \pm 4.2) \times 10^{-2}, \quad 0 < q^2 < 12.6 \text{ GeV}^2, \quad (26)$$

$$\langle A_{\text{FB}}^{\uparrow} \rangle_{\text{SM}}^{\text{high}} = -\mathcal{P}_{\Lambda_b} \times (-5.3 \pm 1.4) \times 10^{-2}, \quad 12.6 \text{ GeV}^2 < q^2 < q_{\text{max}}^2, \quad (27)$$

where “low” and “high” refer to the q^2 regions $0 < q^2 < 12.6 \text{ GeV}^2$ and $12.6 \text{ GeV}^2 < q^2 < q_{\text{max}}^2$, respectively. We find that the uncertainties of the forward-backward asymmetries in the low and high q^2 regions are correlated, with a correlation coefficient of $\rho \simeq +52\%$.

Analogously, we can also obtain SM predictions for the branching ratio in the two different q^2 regions

$$\text{BR}(\Lambda_b \rightarrow \Lambda \nu \bar{\nu})_{\text{SM}}^{\text{low}} = (3.32 \pm 0.99) \times 10^{-6}, \quad 0 < q^2 < 12.6 \text{ GeV}^2, \quad (28)$$

$$\text{BR}(\Lambda_b \rightarrow \Lambda \nu \bar{\nu})_{\text{SM}}^{\text{high}} = (4.39 \pm 0.47) \times 10^{-6}, \quad 12.6 \text{ GeV}^2 < q^2 < q_{\text{max}}^2, \quad (29)$$

with an error correlation of $\rho \simeq +40\%$. The prediction is less precise at low q^2 , because of the larger form factor uncertainties in this kinematic regime.

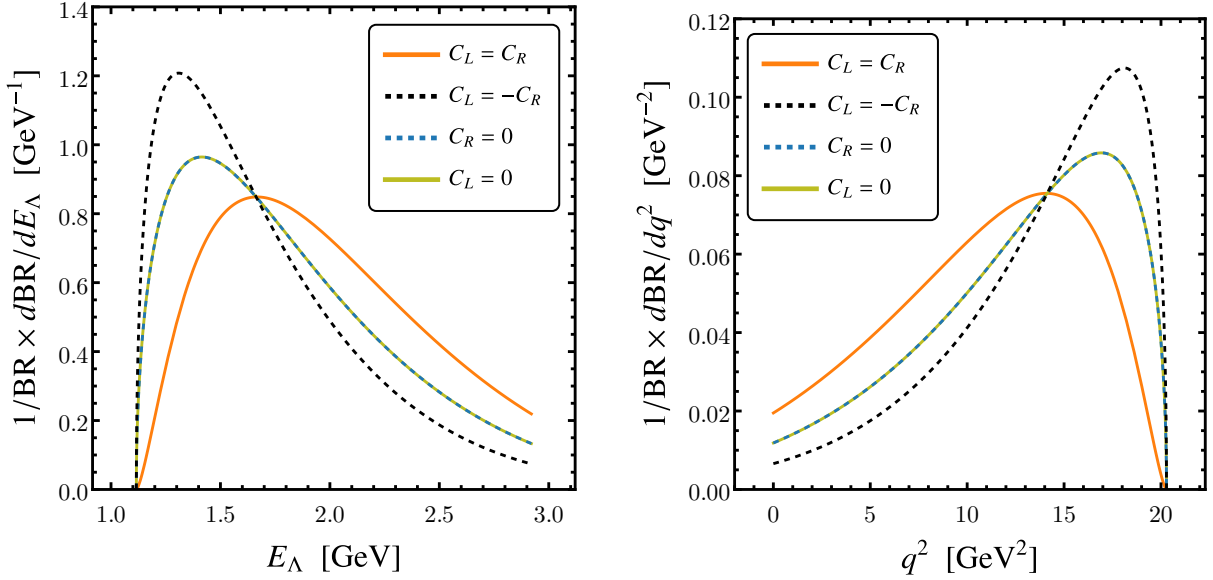


Figure 4. The normalized differential branching ratio of $\Lambda_b \rightarrow \Lambda \nu \bar{\nu}$ in various new physics scenarios as a function of the Λ energy in the Λ_b rest frame E_Λ (left) and the di-neutrino invariant mass squared q^2 (right). The scenario with $C_R = 0$ coincides with the SM prediction.

As we will see below, splitting the phase space into the two q^2 regions below and above the zero crossing of the forward-backward asymmetry enhances the sensitivity to new physics.

B. Impact of Heavy New Physics

In this paper we focus on the impact of heavy new physics on the $\Lambda_b \rightarrow \Lambda \nu \bar{\nu}$ decay. A study of light new physics will be presented elsewhere. Heavy new physics is parameterized by modifications of the two Wilson coefficients C_L and C_R in the effective Hamiltonian, see equation (1). Heavy new physics can change the values of the branching ratio and the forward-backward asymmetry, as well as their kinematic distributions.

In the plots of figure 4, we show the normalized differential branching ratio as a function of the Λ energy (left) and of q^2 (right) in four different new physics scenarios. Scenarios with only left-handed currents ($C_R = 0$, dashed blue) or only right-handed currents ($C_L = 0$, yellow) result in the same kinematic distributions that coincide the SM prediction. Scenarios with vector currents ($C_L = C_R$, orange) give a slightly harder E_Λ spectrum, while the E_Λ spectrum for axial-vector currents ($C_L = -C_R$, dashed black) is slightly softer.

The new physics effects on the forward-backward asymmetry are highly complementary.

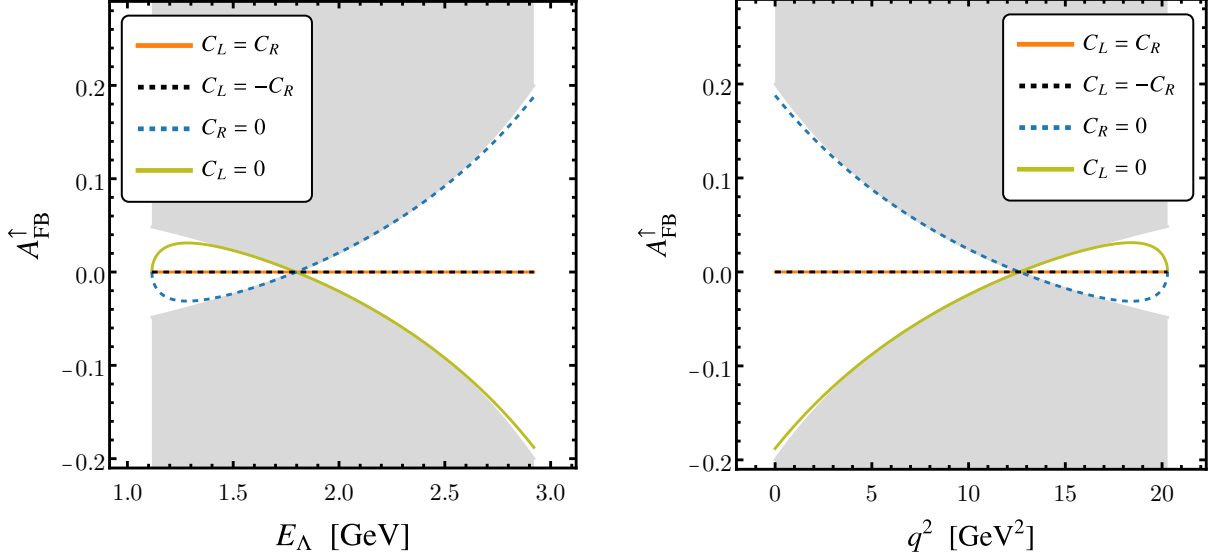


Figure 5. The forward-backward asymmetry in $\Lambda_b \rightarrow \Lambda \nu \bar{\nu}$ in various new physics scenarios as a function of the Λ energy in the Λ_b rest frame E_Λ (left) and the di-neutrino invariant mass squared q^2 (right). The Λ_b polarization is set to its central experimental value $\mathcal{P}_{\Lambda_b} = -0.40$. The scenario with $C_R = 0$ coincides with the SM prediction.

The plots of figure 5 show the forward-backward asymmetry as a function of the Λ energy (left) and of q^2 (right) in the same four new physics scenarios. The forward-backward asymmetry maximally distinguishes the two chiral scenarios $C_R = 0$ and $C_L = 0$. The forward-backward asymmetry vanishes for both the vector and axial-vector scenarios. The gray regions in the plots is theoretically inaccessible. In fact, the maximum value of the forward-backward asymmetry that can in principle be reached is given by

$$|A_{\text{FB}}^\uparrow| < \left| \frac{\mathcal{P}_{\Lambda_b} \mathcal{F}_{VA}}{2\sqrt{\mathcal{F}_V \mathcal{F}_A}} \right|, \quad (30)$$

which defines the boundary of the gray region in the plots of figure 5. In passing, we note that the SM prediction (that coincides with the dashed blue line) is very close to the theoretical maximum of the forward-backward asymmetry.

Interestingly enough, the zero crossing of the forward-backward asymmetry does not change with new physics, but depends purely on form factor inputs. It is always determined by the condition in equation (23). Our predictions in equation (24) therefore serve as an interesting experimental cross-check of the form factor calculations.

IV. SENSITIVITY TO HEAVY NEW PHYSICS

After the discussion in the previous section that focused on the qualitative impact that heavy new physics can have on the $\Lambda_b \rightarrow \Lambda\nu\bar{\nu}$ decay, we now determine quantitatively the sensitivity to heavy new physics.

As discussed above, new physics can modify the value of the branching ratio and the forward-backward asymmetry as well as their kinematic distributions (but not the location of the zero crossing of the forward-backward asymmetry). The new physics sensitivity of the $\Lambda_b \rightarrow \Lambda\nu\bar{\nu}$ observables will depend on the precision of the theory predictions and the uncertainties of the future experimental measurements. The uncertainty of a future $\Lambda_b \rightarrow \Lambda\nu\bar{\nu}$ branching ratio measurement at the FCC-ee was estimated to be around 10% in [77]. This is below the current theory uncertainty of $\sim 14\%$, see equation (20). So far, no estimates exist how well the forward-backward asymmetry could be measured at future Z -pole machines. In our study, we will take into account the current uncertainties on the theory side and will neglect the experimental uncertainties. This illustrates to which extent the current theory precision limits the sensitivity of $\Lambda_b \rightarrow \Lambda\nu\bar{\nu}$. We do expect improved theory predictions by the time the FCC-ee or CEPC would deliver results.

To incorporate new physics to the branching ratio and the forward-backward asymmetry, we find it convenient to normalize the new physics contributions to the Wilson coefficients by the SM Wilson coefficient

$$c_L^{\text{NP}} = C_L^{\text{NP}}/C_L^{\text{SM}} \ , \quad c_R^{\text{NP}} = C_R^{\text{NP}}/C_L^{\text{SM}} \ . \quad (31)$$

The expressions for the branching ratio and the forward-backward asymmetry in the presence of new physics are then

$$\text{BR}(\Lambda_b \rightarrow \Lambda\nu\bar{\nu}) = \text{BR}(\Lambda_b \rightarrow \Lambda\nu\bar{\nu})_{\text{SM}} \left(r|1 + c_L^{\text{NP}} + c_R^{\text{NP}}|^2 + (1-r)|1 + c_L^{\text{NP}} - c_R^{\text{NP}}|^2 \right) \quad (32)$$

$$\langle A_{\text{FB}}^\uparrow \rangle = \frac{\langle A_{\text{FB}}^\uparrow \rangle_{\text{SM}} \left(|1 + c_L^{\text{NP}}|^2 - |c_R^{\text{NP}}|^2 \right)}{r|1 + c_L^{\text{NP}} + c_R^{\text{NP}}|^2 + (1-r)|1 + c_L^{\text{NP}} - c_R^{\text{NP}}|^2} \ , \quad (33)$$

where the parameter r is given by

$$r = \frac{\int_{E_\Lambda^{\text{min}}}^{E_\Lambda^{\text{max}}} dE_\Lambda E_\Lambda^2 \sqrt{1 - \frac{m_\Lambda^2}{E_\Lambda^2}} \mathcal{F}_V}{\int_{E_\Lambda^{\text{min}}}^{E_\Lambda^{\text{max}}} dE_\Lambda E_\Lambda^2 \sqrt{1 - \frac{m_\Lambda^2}{E_\Lambda^2}} (\mathcal{F}_V + \mathcal{F}_A)} \ . \quad (34)$$

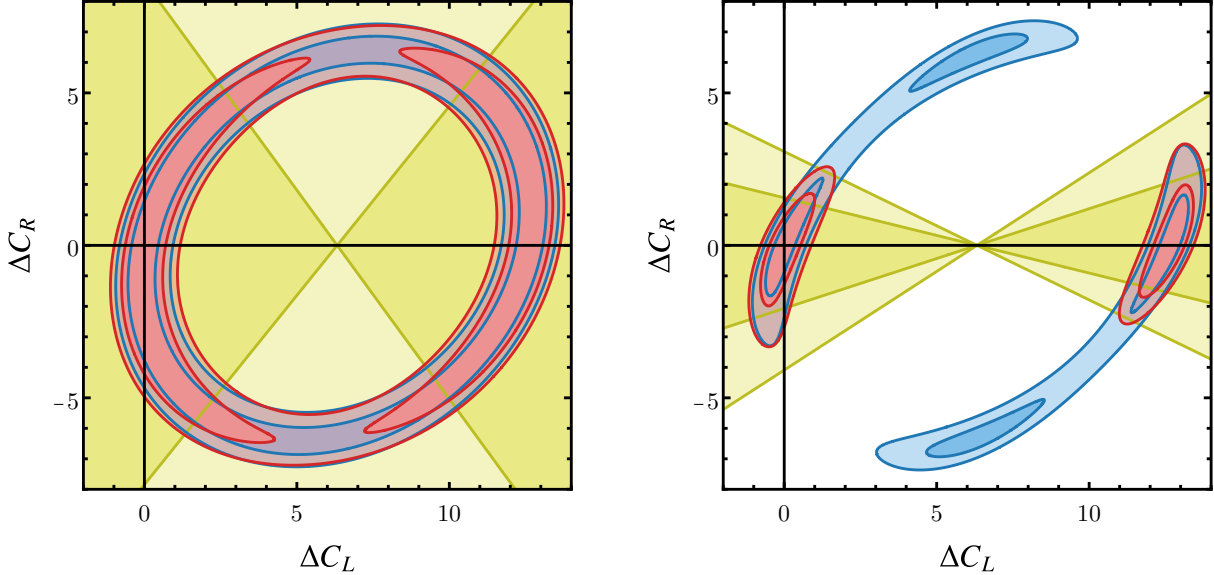


Figure 6. The expected sensitivity of $\Lambda_b \rightarrow \Lambda \nu \bar{\nu}$ to new physics parameterized by the Wilson coefficients C_L^{NP} and C_R^{NP} . Left: taking into account a single large q^2 bin; Right: splitting the q^2 range into two bins, one above and one below the zero crossing of the forward-backward asymmetry. The blue, yellow, and red regions correspond to the constraints from the branching ratio, the forward-backward asymmetry, and their combination, respectively. Dark and light shaded regions indicate 1σ and 2σ constraints.

The expressions can be applied for any range of the Λ energy or q^2 , respectively. In particular, we find for the total q^2 range and the low and high q^2 ranges

$$r_{\text{tot}} \simeq 0.41, \quad r_{\text{low}} \simeq 0.55, \quad r_{\text{high}} \simeq 0.30. \quad (35)$$

In figure 6, we show the allowed regions in C_L^{NP} vs. C_R^{NP} parameter space, assuming that the experimental measurements of the branching ratio and the forward-backward asymmetry agree precisely with our SM predictions. The plot on the left takes into account observables integrated over the full q^2 range, while in the plot on the right we include the low and high q^2 regions separately, taking into account their correlations. We assume that both C_L^{NP} and C_R^{NP} are real.

The blue regions correspond to the constraint we anticipate from a future branching ratio measurement at the 1σ and 2σ level, while the yellow regions correspond to a measurement of the forward-backward asymmetry. The red regions show the combination of both. More precisely, the dark and light shaded regions correspond to a $\Delta\chi^2$ of 1 and 4, when we

consider the branching ratio or the forward backward asymmetry individually (blue and yellow regions), and to a $\Delta\chi^2$ of 2.3 and 6 in the combination (red regions). As expected, the branching ratio and the forward-backward asymmetry have complementary sensitivity. However, if the forward-backward asymmetry is integrated over the entire q^2 range, its constraining power is largely washed out. A much better sensitivity is obtained if the high- q^2 and low- q^2 regions are taken into account separately, which avoids cancellations in the forward-backward asymmetry.

In the right plot, we observe two clearly resolved regions of parameter space: one in the vicinity of the SM point $C_L^{\text{NP}} = C_R^{\text{NP}} = 0$, and one with $C_L^{\text{NP}} \simeq -2C_L^{\text{SM}} \simeq 12.6$, $C_R^{\text{NP}} \simeq 0$. The second region corresponds to a total $b \rightarrow s\nu\nu$ amplitude with opposite sign compared to the SM, a scenario that cannot be distinguished from the SM using only $b \rightarrow s\nu\nu$ decays. We consider such a scenario contrived and do not discuss it further.

We can translate the allowed region around the point $C_L^{\text{NP}} = C_R^{\text{NP}} = 0$ into constraints on the new physics scale, using the parameterization

$$\frac{1}{\Lambda_L^2} = \frac{4G_F}{\sqrt{2}} \frac{\alpha}{4\pi} |V_{ts}^* V_{tb}| C_L^{\text{NP}}, \quad \frac{1}{\Lambda_R^2} = \frac{4G_F}{\sqrt{2}} \frac{\alpha}{4\pi} |V_{ts}^* V_{tb}| C_R^{\text{NP}}. \quad (36)$$

We find the following 2σ limits

$$\frac{-1}{(45 \text{ TeV})^2} \lesssim \frac{1}{\Lambda_L^2} \lesssim \frac{1}{(44 \text{ TeV})^2}, \quad \frac{-1}{(25 \text{ TeV})^2} \lesssim \frac{1}{\Lambda_R^2} \lesssim \frac{1}{(33 \text{ TeV})^2}. \quad (37)$$

These new physics scales are in the same ballpark as the scales that are probed by $b \rightarrow s\mu\mu$ decays (see e.g. [122, 123]) and by the rare meson decays with neutrinos in the final state $B \rightarrow K\nu\bar{\nu}$ and $B \rightarrow K^*\nu\bar{\nu}$ (see e.g. [50, 51]).

V. DIFFERENTIAL BRANCHING RATIO IN THE LAB FRAME

As we have seen in the previous section, a measurement of the forward-backward asymmetry provides interesting sensitivity to new physics that is complementary to measurements of the branching ratio. We note that a measurement of A_{FB}^\uparrow requires access to the angle between the flight direction of the Λ in the Λ_b rest frame and the flight direction of the Λ_b in the lab frame. Reconstructing the Λ_b rest frame might be challenging due to the two neutrinos in the decay², and we therefore explore to which extent information about the

² One could for example estimate the di-neutrino energy and momentum using the missing energy and momentum in the hemisphere containing the Λ_b .

forward-backward asymmetry (or, equivalently, information about the chirality structure of the $b \rightarrow s\nu\nu$ transition) can be extracted from lab frame observables alone. The approach is inspired by methods to determine the Λ_b polarization at LEP, using semi-leptonic decays [78, 117, 118].

For the following, it will be useful to introduce the shorthand notation

$$\hat{\beta}_{\Lambda_b} = \sqrt{1 - \frac{m_{\Lambda_b}^2}{\hat{E}_{\Lambda_b}^2}}, \quad \hat{\beta}_{\Lambda} = \sqrt{1 - \frac{m_{\Lambda}^2}{\hat{E}_{\Lambda}^2}}, \quad \beta_{\Lambda} = \sqrt{1 - \frac{m_{\Lambda}^2}{E_{\Lambda}^2}}, \quad (38)$$

where $\hat{\beta}_{\Lambda_b}$ is the velocity of the Λ_b in the lab frame, $\hat{\beta}_{\Lambda}$ the velocity of the Λ in the lab frame, and β_{Λ} the velocity of the Λ in the Λ_b restframe, respectively.

The relevant lab frame observable is the differential decay rate as a function of the Λ energy in the lab frame that we denote with \hat{E}_{Λ} . We find

$$\frac{d\text{BR}(\Lambda_b \rightarrow \Lambda\nu\bar{\nu})}{d\hat{E}_{\Lambda}} = \int_{E_{\Lambda}^{\min}}^{E_{\Lambda}^{\max}} \frac{dE_{\Lambda}}{E_{\Lambda}} \frac{m_{\Lambda_b}}{\hat{E}_{\Lambda_b}} \frac{1}{\hat{\beta}_{\Lambda_b}\beta_{\Lambda}} \frac{d\text{BR}(\Lambda_b \rightarrow \Lambda\nu\bar{\nu})}{dE_{\Lambda}d\cos\theta_{\Lambda}}, \quad (39)$$

where \hat{E}_{Λ_b} is the energy of the Λ_b in the lab frame, and in the expression for the differential branching ratio in the Λ_b restframe (9), one needs to replace

$$\cos\theta_{\Lambda} = \frac{1}{\hat{\beta}_{\Lambda_b}\beta_{\Lambda}} \left(\frac{\hat{E}_{\Lambda}}{E_{\Lambda}} \frac{m_{\Lambda_b}}{\hat{E}_{\Lambda_b}} - 1 \right). \quad (40)$$

The lower and upper integration boundaries in (39) are given by

$$E_{\Lambda}^{\min} = \frac{\hat{E}_{\Lambda}\hat{E}_{\Lambda_b}}{m_{\Lambda_b}} \left(1 - \hat{\beta}_{\Lambda_b}\hat{\beta}_{\Lambda} \right), \quad (41)$$

$$E_{\Lambda}^{\max} = \text{Min} \left\{ \frac{m_{\Lambda_b}}{2} (1 + x_{\Lambda}^2), \frac{\hat{E}_{\Lambda}\hat{E}_{\Lambda_b}}{m_{\Lambda_b}} \left(1 + \hat{\beta}_{\Lambda_b}\hat{\beta}_{\Lambda} \right) \right\}. \quad (42)$$

The physical range of the Λ energy in the lab frame is

$$\hat{E}_{\Lambda}^{\min} = \begin{cases} m_{\Lambda} & \text{if } \hat{\beta}_{\Lambda_b} < \frac{1 - x_{\Lambda}^2}{1 + x_{\Lambda}^2}, \\ \frac{\hat{E}_{\Lambda_b}}{2} \left(1 + x_{\Lambda}^2 - (1 - x_{\Lambda}^2) \hat{\beta}_{\Lambda_b} \right) & \text{if } \hat{\beta}_{\Lambda_b} > \frac{1 - x_{\Lambda}^2}{1 + x_{\Lambda}^2}, \end{cases} \quad (43)$$

$$\hat{E}_{\Lambda}^{\max} = \frac{\hat{E}_{\Lambda_b}}{2} \left(1 + x_{\Lambda}^2 + (1 - x_{\Lambda}^2) \hat{\beta}_{\Lambda_b} \right). \quad (44)$$

The \hat{E}_{Λ} spectrum depends on \hat{E}_{Λ_b} , the energy of the decaying Λ_b . The energy spectrum of B mesons produced on the Z -pole has been measured at LEP [124]. The average energy

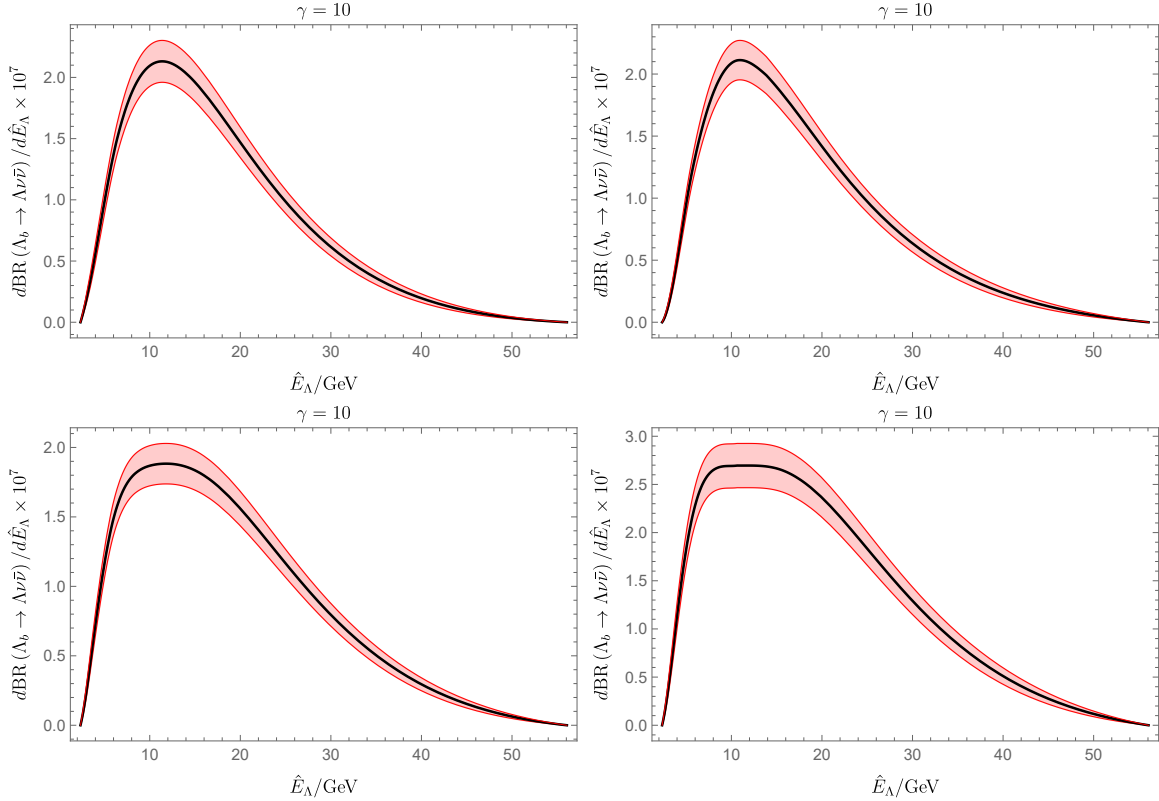


Figure 7. The differential branching ratio $\Lambda_b \rightarrow \Lambda \nu \bar{\nu}$ as a function of the Λ energy in the lab frame. For illustration, we set the Λ_b energy to $\hat{E}_{\Lambda_b} = 10 m_{\Lambda_b} \simeq 56$ GeV. We show a few benchmark cases: $C_L = C_L^{\text{SM}}, C_R = 0$ (top left), $C_L = 0, C_R = C_L^{\text{SM}}$ (top right), $C_L = 2C_R = C_L^{\text{SM}}$ (bottom left), and $C_L = C_R = C_L^{\text{SM}}$ (bottom right). The shaded band corresponds to the 1σ theory uncertainty on the branching ratio.

is around 70% of half the center of mass energy. As argued in [118] the average energies of mesons and baryons should be very similar and we therefore expect an average energy of Λ_b baryons of around (30-35) GeV, however, with a distribution that covers also much smaller and much larger values.

We find that the differential branching ratio (39) scales to a very good approximation with the Λ_b energy, i.e. its shape is approximately invariant if plotted as a function of $\hat{E}_\Lambda / \hat{E}_{\Lambda_b}$. For illustration, we show in figure 7 the differential branching ratio as a function of the Λ energy in the lab frame for a fixed $\hat{E}_{\Lambda_b} = 10 m_{\Lambda_b} \simeq 56$ GeV. The four panels correspond to four benchmark cases for the Wilson coefficients: $C_L = C_L^{\text{SM}}, C_R = 0$ (top left), $C_L = 0, C_R = C_L^{\text{SM}}$ (top right), $C_L = 2C_R = C_L^{\text{SM}}$ (bottom left), and $C_L = C_R = C_L^{\text{SM}}$ (bottom right). The peak of the distributions is at a Λ energy of around $\hat{E}_\Lambda \simeq 0.2 \times \hat{E}_{\Lambda_b}$ in all cases.

The distribution is much broader if both C_L and C_R are present.

The distributions for purely left-chiral interactions (top left) and purely right-chiral interactions (top right) are very similar. This result indicates that the effect of the forward backward asymmetry (that maximally distinguishes between the left-chiral and right-chiral scenarios, see figure 5) is largely washed out in the lab frame. Dedicated sensitivity studies are required to determine to which extent a lab frame analysis could recover information about the chirality structure, or if a Λ_b rest frame analysis can provide much better sensitivity.

VI. CONCLUSIONS

In this paper, we explored the new physics sensitivity of the rare decay $\Lambda_b \rightarrow \Lambda \nu \bar{\nu}$. The decay has never been observed but can be accessed at future Z -pole machines like FCC-ee and CEPC. In contrast to the mesonic counterparts ($B \rightarrow K \nu \bar{\nu}$, $B \rightarrow K^* \nu \bar{\nu}$, and $B_s \rightarrow \phi \nu \bar{\nu}$), Λ_b baryons produced in Z decays are longitudinally polarized, which offers complementary novel observables to test the Standard Model.

The kinematics of the Λ baryon in the final state depends on two independent variables, its energy and the angle between its momentum and the spin of the Λ_b . We find that the corresponding angular decay distribution is characterized by a forward-backward asymmetry, A_{FB}^\uparrow , that is proportional to the longitudinal polarization of the Λ_b . We give state-of-the-art predictions for the integrated branching ratio, $\text{BR}(\Lambda_b \rightarrow \Lambda \nu \bar{\nu})$, and the forward-backward asymmetry, A_{FB}^\uparrow , in the Standard Model. The uncertainties are dominated by the current knowledge of $\Lambda_b \rightarrow \Lambda$ form factors, providing continued motivation to improve baryon form factor calculations on the lattice. We find that the forward-backward asymmetry has a zero crossing at a specific value of the Λ energy, E_Λ (or equivalently of the di-neutrino invariant mass, q^2). Interestingly, the location of the zero-crossing is independent of new physics and therefore can be used as an experimental test of form factor calculations. On the other hand, the q^2 shapes of the differential branching ratio and the forward-backward asymmetry do depend on new physics.

Parameterizing heavy new physics in $\Lambda_b \rightarrow \Lambda \nu \bar{\nu}$ by an effective Hamiltonian, we determine the expected new physics sensitivity of future precision measurements of $\Lambda_b \rightarrow \Lambda \nu \bar{\nu}$ on the Z -pole. We find that splitting the q^2 region into two bins, one above the A_{FB}^\uparrow zero crossing and

one below, greatly enhances the new physics sensitivity, and allows one to break degeneracies in the new physics parameter space. We find that new physics scales of $\Lambda_{\text{NP}} \sim (25 - 45)$ TeV can be probed. This is comparable to the scales that can be probed with other $b \rightarrow s\nu\bar{\nu}$ decays and with $b \rightarrow s\ell^+\ell^-$ decays. It would be interesting to extend our study to the $\Lambda_b \rightarrow \Lambda\ell^+\ell^-$ decays on the Z -pole. Also in that case we expect that the longitudinal polarization of the Λ_b gives novel probes of new physics.

An experimental measurement of the forward-backward asymmetry requires reconstruction of the Λ_b rest frame. Because of the presence of the two neutrinos in the final state, this may be challenging. We therefore also explored to which extent information about the forward-backward asymmetry can be accessed from lab frame observables. We find that different values of the forward-backward asymmetry leave only a very mild imprint on the energy distribution of the Λ in the lab frame. More detailed studies are required to determine if a lab frame analysis or a Λ_b rest frame analysis would have better sensitivities.

ACKNOWLEDGEMENTS

We thank Howard Haber and Jason Nielsen for useful discussions. The research of WA, SAG, and KT is supported by the U.S. Department of Energy grant number DE-SC0010107.

Appendix A: Form Factors

In this appendix we give details about our implementation of the $\Lambda_b \rightarrow \Lambda$ form factors. We follow [94] and parameterize the form factors using a z -expansion

$$f(q^2) = \frac{1}{1 - q^2/(m_{\text{pole}}^f)^2} \sum_n a_n^f z^n, \quad z = \frac{\sqrt{t_+ - q^2} - \sqrt{t_+ - t_0}}{\sqrt{t_+ - q^2} + \sqrt{t_+ - t_0}}. \quad (\text{A1})$$

The parameters t_0 and t_+ are chosen such that the kinematic endpoint q_{max}^2 is mapped to $z = 0$, and q^2 values above the BK threshold are mapped onto the unit circle in the complex z plane

$$t_0 = (m_{\Lambda_b} - m_{\Lambda})^2, \quad t_+ = (m_B + m_K)^2. \quad (\text{A2})$$

The poles that correspond to the lowest relevant B_s mesons are factored out explicitly. The corresponding masses m_{pole}^f and the expansion coefficients a_n^f are taken from [94].

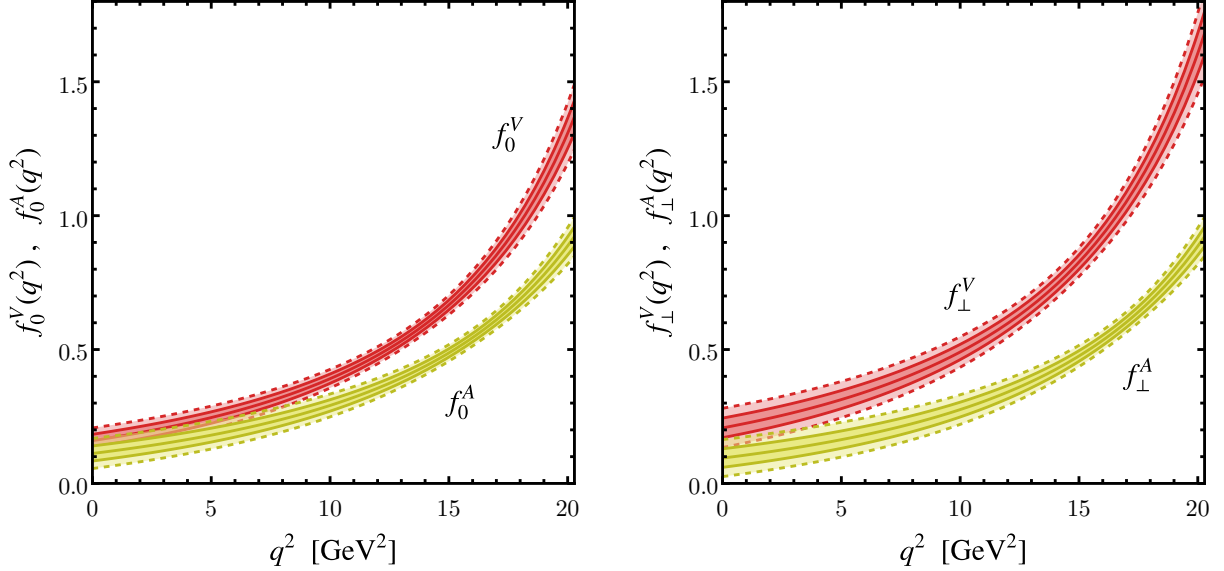


Figure 8. The relevant $\Lambda_b \rightarrow \Lambda$ form factors as a function of q^2 . The colored bands correspond to the 1σ and 2σ uncertainties.

To obtain the form factor uncertainties, we follow the procedure recommended in [94] that takes into account the difference in the results based on z -expansions up to order $n = 1$ and $n = 2$. Figure 8 shows all the form factors relevant for our analysis with their 1σ and 2σ uncertainties.

-
- [1] T. Blake, G. Lanfranchi and D.M. Straub, *Rare B Decays as Tests of the Standard Model*, *Prog. Part. Nucl. Phys.* **92** (2017) 50 [[1606.00916](#)].
 - [2] W. Altmannshofer and F. Archilli, *Rare decays of b and c hadrons*, in *Snowmass 2021*, 6, 2022 [[2206.11331](#)].
 - [3] LHCb collaboration, *Differential branching fractions and isospin asymmetries of $B \rightarrow K^{(*)}\mu^+\mu^-$ decays*, *JHEP* **06** (2014) 133 [[1403.8044](#)].
 - [4] LHCb collaboration, *Measurements of the S-wave fraction in $B^0 \rightarrow K^+\pi^-\mu^+\mu^-$ decays and the $B^0 \rightarrow K^*(892)^0\mu^+\mu^-$ differential branching fraction*, *JHEP* **11** (2016) 047 [[1606.04731](#)].
 - [5] LHCb collaboration, *Branching Fraction Measurements of the Rare $B_s^0 \rightarrow \phi\mu^+\mu^-$ and $B_s^0 \rightarrow f_2'(1525)\mu^+\mu^-$ Decays*, *Phys. Rev. Lett.* **127** (2021) 151801 [[2105.14007](#)].

- [6] LHCb collaboration, *Angular analysis of the $B^0 \rightarrow K^{*0} \mu^+ \mu^-$ decay using 3 fb⁻¹ of integrated luminosity*, *JHEP* **02** (2016) 104 [[1512.04442](#)].
- [7] CMS collaboration, *Measurement of angular parameters from the decay $B^0 \rightarrow K^{*0} \mu^+ \mu^-$ in proton-proton collisions at $\sqrt{s} = 8$ TeV*, *Phys. Lett. B* **781** (2018) 517 [[1710.02846](#)].
- [8] ATLAS collaboration, *Angular analysis of $B_d^0 \rightarrow K^* \mu^+ \mu^-$ decays in pp collisions at $\sqrt{s} = 8$ TeV with the ATLAS detector*, *JHEP* **10** (2018) 047 [[1805.04000](#)].
- [9] LHCb collaboration, *Measurement of CP-Averaged Observables in the $B^0 \rightarrow K^{*0} \mu^+ \mu^-$ Decay*, *Phys. Rev. Lett.* **125** (2020) 011802 [[2003.04831](#)].
- [10] LHCb collaboration, *Angular Analysis of the $B^+ \rightarrow K^{*+} \mu^+ \mu^-$ Decay*, *Phys. Rev. Lett.* **126** (2021) 161802 [[2012.13241](#)].
- [11] LHCb collaboration, *Angular analysis of the rare decay $B_s^0 \rightarrow \phi \mu^+ \mu^-$* , *JHEP* **11** (2021) 043 [[2107.13428](#)].
- [12] LHCb collaboration, *Determination of short- and long-distance contributions in $B^0 \rightarrow K^{*0} \mu^+ \mu^-$ decays*, *Phys. Rev. D* **109** (2024) 052009 [[2312.09102](#)].
- [13] LHCb collaboration, *Amplitude Analysis of the $B^0 \rightarrow K^{*0} \mu^+ \mu^-$ Decay*, *Phys. Rev. Lett.* **132** (2024) 131801 [[2312.09115](#)].
- [14] LHCb collaboration, *Comprehensive analysis of local and nonlocal amplitudes in the $B^0 \rightarrow K^{*0} \mu^+ \mu^-$ decay*, *JHEP* **09** (2024) 026 [[2405.17347](#)].
- [15] CMS collaboration, *Angular analysis of the $B^0 \rightarrow K^*(892)^0 \mu^+ \mu^-$ decay in proton-proton collisions at $\sqrt{s} = 13$ TeV*, [2411.11820](#).
- [16] LHCb collaboration, *Tests of lepton universality using $B^0 \rightarrow K_S^0 \ell^+ \ell^-$ and $B^+ \rightarrow K^{*+} \ell^+ \ell^-$ decays*, *Phys. Rev. Lett.* **128** (2022) 191802 [[2110.09501](#)].
- [17] LHCb collaboration, *Test of lepton universality in $b \rightarrow s \ell^+ \ell^-$ decays*, *Phys. Rev. Lett.* **131** (2023) 051803 [[2212.09152](#)].
- [18] LHCb collaboration, *Measurement of lepton universality parameters in $B^+ \rightarrow K^+ \ell^+ \ell^-$ and $B^0 \rightarrow K^{*0} \ell^+ \ell^-$ decays*, *Phys. Rev. D* **108** (2023) 032002 [[2212.09153](#)].
- [19] CMS collaboration, *Test of lepton flavor universality in $B^\pm \rightarrow K^\pm \mu^+ \mu^-$ and $B^\pm \rightarrow K^\pm e^+ e^-$ decays in proton-proton collisions at $\sqrt{s} = 13$ TeV*, *Rept. Prog. Phys.* **87** (2024) 077802 [[2401.07090](#)].
- [20] LHCb collaboration, *Test of lepton flavour universality with $B_s^0 \rightarrow \phi \ell^+ \ell^-$ decays*, [2410.13748](#).

- [21] W. Altmannshofer and P. Stangl, *New physics in rare B decays after Moriond 2021*, *Eur. Phys. J. C* **81** (2021) 952 [2103.13370].
- [22] N.R. Singh Chundawat, *CP violation in $b \rightarrow s\ell\ell$: a model independent analysis*, *Phys. Rev. D* **107** (2023) 075014 [2207.10613].
- [23] M. Ciuchini, M. Fedele, E. Franco, A. Paul, L. Silvestrini and M. Valli, *Constraints on lepton universality violation from rare B decays*, *Phys. Rev. D* **107** (2023) 055036 [2212.10516].
- [24] A. Greljo, J. Salko, A. Smolkovič and P. Stangl, *Rare b decays meet high-mass Drell-Yan*, *JHEP* **05** (2023) 087 [2212.10497].
- [25] M. Algueró, A. Biswas, B. Capdevila, S. Descotes-Genon, J. Matias and M. Novoa-Brunet, *To (b)e or not to (b)e: no electrons at LHCb*, *Eur. Phys. J. C* **83** (2023) 648 [2304.07330].
- [26] Q. Wen and F. Xu, *Global fits of new physics in $b \rightarrow s$ after the $R_{K^{(*)}}$ 2022 release*, *Phys. Rev. D* **108** (2023) 095038 [2305.19038].
- [27] W. Altmannshofer, S.A. Gadam and S. Profumo, *Probing new physics with $\mu^+\mu^- \rightarrow bs$ at a muon collider*, *Phys. Rev. D* **108** (2023) 115033 [2306.15017].
- [28] D. Guadagnoli, C. Normand, S. Simula and L. Vittorio, *Insights on the current semi-leptonic B-decay discrepancies and how $B_s \rightarrow \mu^+\mu^-\gamma$ can help*, *JHEP* **10** (2023) 102 [2308.00034].
- [29] T. Hurth, F. Mahmoudi and S. Neshatpour, *B anomalies in the post $R_{K^{(*)}}$ era*, *Phys. Rev. D* **108** (2023) 115037 [2310.05585].
- [30] M. Bordone, G. Isidori, S. Mächler and A. Tinari, *Short- vs. long-distance physics in $B \rightarrow K^{(*)}\ell^+\ell^-$: a data-driven analysis*, *Eur. Phys. J. C* **84** (2024) 547 [2401.18007].
- [31] R.R. Horgan, Z. Liu, S. Meinel and M. Wingate, *Calculation of $B^0 \rightarrow K^{*0}\mu^+\mu^-$ and $B_s^0 \rightarrow \phi\mu^+\mu^-$ observables using form factors from lattice QCD*, *Phys. Rev. Lett.* **112** (2014) 212003 [1310.3887].
- [32] HPQCD collaboration, *Rare decay $B \rightarrow K\ell^+\ell^-$ form factors from lattice QCD*, *Phys. Rev. D* **88** (2013) 054509 [1306.2384].
- [33] R.R. Horgan, Z. Liu, S. Meinel and M. Wingate, *Rare B decays using lattice QCD form factors*, *PoS LATTICE2014* (2015) 372 [1501.00367].
- [34] J.A. Bailey et al., *$B \rightarrow K\ell^+\ell^-$ Decay Form Factors from Three-Flavor Lattice QCD*, *Phys. Rev. D* **93** (2016) 025026 [1509.06235].

- [35] N. Gubernari, A. Kokulu and D. van Dyk, *B → P and B → V Form Factors from B-Meson Light-Cone Sum Rules beyond Leading Twist*, *JHEP* **01** (2019) 150 [1811.00983].
- [36] N. Gubernari, M. Reboud, D. van Dyk and J. Virto, *Improved theory predictions and global analysis of exclusive $b \rightarrow s\mu^+\mu^-$ processes*, *JHEP* **09** (2022) 133 [2206.03797].
- [37] N. Gubernari, M. Reboud, D. van Dyk and J. Virto, *Dispersive analysis of $B \rightarrow K^{(*)}$ and $B_s \rightarrow \phi$ form factors*, *JHEP* **12** (2023) 153 [2305.06301].
- [38] T.M. Aliev, K. Azizi and M. Savci, *Analysis of the $\Lambda_b \rightarrow \Lambda\ell^+\ell^-$ decay in QCD*, *Phys. Rev. D* **81** (2010) 056006 [1001.0227].
- [39] W. Altmannshofer, A.J. Buras, D.M. Straub and M. Wick, *New strategies for New Physics search in $B \rightarrow K^*\nu\bar{\nu}$, $B \rightarrow K\nu\bar{\nu}$ and $B \rightarrow X_s\nu\bar{\nu}$ decays*, *JHEP* **04** (2009) 022 [0902.0160].
- [40] A.J. Buras, J. Girrbach-Noe, C. Niehoff and D.M. Straub, *$B \rightarrow K^{(*)}\nu\bar{\nu}$ decays in the Standard Model and beyond*, *JHEP* **02** (2015) 184 [1409.4557].
- [41] T.E. Browder, N.G. Deshpande, R. Mandal and R. Sinha, *Impact of $B \rightarrow K\nu\bar{\nu}$ measurements on beyond the Standard Model theories*, *Phys. Rev. D* **104** (2021) 053007 [2107.01080].
- [42] R. Bause, H. Gisbert, M. Golz and G. Hiller, *Interplay of dineutrino modes with semileptonic rare B-decays*, *JHEP* **12** (2021) 061 [2109.01675].
- [43] D. Bečirević, G. Piazza and O. Sumensari, *Revisiting $B \rightarrow K^{(*)}\nu\bar{\nu}$ decays in the Standard Model and beyond*, *Eur. Phys. J. C* **83** (2023) 252 [2301.06990].
- [44] N. Rajeev and R. Dutta, *Consequences of $b \rightarrow s\mu^+\mu^-$ anomalies on $B \rightarrow K^{(*)}\nu\bar{\nu}$, $B_s \rightarrow (\eta, \eta')\nu\bar{\nu}$ and $B_s \rightarrow \phi\nu\bar{\nu}$ decay observables*, *Phys. Rev. D* **105** (2022) 115028 [2112.11682].
- [45] BABAR collaboration, *Search for the Rare Decay $B \rightarrow K\nu\bar{\nu}$* , *Phys. Rev. D* **82** (2010) 112002 [1009.1529].
- [46] BELLE collaboration, *Search for $B \rightarrow h^{(*)}\nu\bar{\nu}$ with the full Belle $\Upsilon(4S)$ data sample*, *Phys. Rev. D* **87** (2013) 111103 [1303.3719].
- [47] BABAR collaboration, *Search for $B \rightarrow K^{(*)}\nu\bar{\nu}$ and invisible quarkonium decays*, *Phys. Rev. D* **87** (2013) 112005 [1303.7465].
- [48] BELLE collaboration, *Search for $B \rightarrow h\nu\bar{\nu}$ decays with semileptonic tagging at Belle*, *Phys. Rev. D* **96** (2017) 091101 [1702.03224].

- [49] BELLE-II collaboration, *Evidence for $B^+ \rightarrow K^+\nu\bar{\nu}$ decays*, *Phys. Rev. D* **109** (2024) 112006 [2311.14647].
- [50] R. Bause, H. Gisbert and G. Hiller, *Implications of an enhanced $B \rightarrow K\nu\bar{\nu}$ branching ratio*, *Phys. Rev. D* **109** (2024) 015006 [2309.00075].
- [51] L. Allwicher, D. Becirevic, G. Piazza, S. Rosauero-Alcaraz and O. Sumensari, *Understanding the first measurement of $B(B \rightarrow K\nu\bar{\nu})$* , *Phys. Lett. B* **848** (2024) 138411 [2309.02246].
- [52] T. Felkl, A. Giri, R. Mohanta and M.A. Schmidt, *When energy goes missing: new physics in $b \rightarrow s\nu\bar{\nu}$ with sterile neutrinos*, *Eur. Phys. J. C* **83** (2023) 1135 [2309.02940].
- [53] H.K. Dreiner, J.Y. Günther and Z.S. Wang, *The Decay $B \rightarrow K\nu\bar{\nu}$ at Belle II and a Massless Bino in R-parity-violating Supersymmetry*, 2309.03727.
- [54] X.-G. He, X.-D. Ma and G. Valencia, *Revisiting models that enhance $B^+ \rightarrow K^+\nu\bar{\nu}$ in light of the new Belle II measurement*, *Phys. Rev. D* **109** (2024) 075019 [2309.12741].
- [55] A. Berezhnoy and D. Melikhov, *$B \rightarrow K^*M_X$ vs $B \rightarrow KM_X$ as a probe of a scalar-mediator dark matter scenario*, *EPL* **145** (2024) 14001 [2309.17191].
- [56] A. Datta, D. Marfatia and L. Mukherjee, *$B \rightarrow K\nu\bar{\nu}$, MiniBooNE and muon $g-2$ anomalies from a dark sector*, *Phys. Rev. D* **109** (2024) L031701 [2310.15136].
- [57] W. Altmannshofer, A. Crivellin, H. Haigh, G. Inguglia and J. Martin Camalich, *Light new physics in $B \rightarrow K^{(*)}\nu\bar{\nu}$?*, *Phys. Rev. D* **109** (2024) 075008 [2311.14629].
- [58] D. McKeen, J.N. Ng and D. Tuckler, *Higgs portal interpretation of the Belle II $B^+ \rightarrow K^+\nu\bar{\nu}$ measurement*, *Phys. Rev. D* **109** (2024) 075006 [2312.00982].
- [59] K. Fridell, M. Ghosh, T. Okui and K. Tobioka, *Decoding the $B \rightarrow K\nu\bar{\nu}$ excess at Belle II: Kinematics, operators, and masses*, *Phys. Rev. D* **109** (2024) 115006 [2312.12507].
- [60] S.-Y. Ho, J. Kim and P. Ko, *Recent $B^+ \rightarrow K^+\nu\bar{\nu}$ Excess and Muon $g - 2$ Illuminating Light Dark Sector with Higgs Portal*, 2401.10112.
- [61] F.-Z. Chen, Q. Wen and F. Xu, *Correlating $B \rightarrow K^{(*)}\nu\bar{\nu}$ and flavor anomalies in SMEFT*, *Eur. Phys. J. C* **84** (2024) 1012 [2401.11552].
- [62] E. Gabrielli, L. Marzola, K. Mürsepp and M. Raidal, *Explaining the $B^+ \rightarrow K^+\nu\bar{\nu}$ excess via a massless dark photon*, *Eur. Phys. J. C* **84** (2024) 460 [2402.05901].
- [63] B.-F. Hou, X.-Q. Li, M. Shen, Y.-D. Yang and X.-B. Yuan, *Deciphering the Belle II data on $B \rightarrow K\nu\bar{\nu}$ decay in the (dark) SMEFT with minimal flavour violation*, *JHEP* **06** (2024) 172 [2402.19208].

- [64] X.-G. He, X.-D. Ma, M.A. Schmidt, G. Valencia and R.R. Volkas, *Scalar dark matter explanation of the excess in the Belle II $B^+ \rightarrow K^+ + \text{invisible}$ measurement*, *JHEP* **07** (2024) 168 [[2403.12485](#)].
- [65] P.D. Bolton, S. Fajfer, J.F. Kamenik and M. Novoa-Brunet, *Signatures of light new particles in $B \rightarrow K^{(*)} + E_{\text{miss}}$* , *Phys. Rev. D* **110** (2024) 055001 [[2403.13887](#)].
- [66] D. Marzocca, M. Nardecchia, A. Stanzione and C. Toni, *Implications of $B \rightarrow K\nu\bar{\nu}$ under rank-one flavor violation hypothesis*, *Eur. Phys. J. C* **84** (2024) 1217 [[2404.06533](#)].
- [67] A.J. Buras, J. Harz and M.A. Mojahed, *Disentangling new physics in $K \rightarrow \pi\nu\bar{\nu}$ and $B \rightarrow K(K^*)\nu\bar{\nu}$ observables*, *JHEP* **10** (2024) 087 [[2405.06742](#)].
- [68] L. Allwicher, M. Bordone, G. Isidori, G. Piazza and A. Stanzione, *Probing third-generation New Physics with $K \rightarrow \pi\nu\bar{\nu}$ and $B \rightarrow K^{(*)}\nu\bar{\nu}$* , [2410.21444](#).
- [69] W. Altmannshofer and S. Roy, *A joint explanation of the $B \rightarrow \pi K$ puzzle and the $B \rightarrow K\nu\bar{\nu}$ excess*, [2411.06592](#).
- [70] Q.-Y. Hu, *Are the new particles heavy or light in $b \rightarrow sE_{\text{miss}}$?*, [2412.19084](#).
- [71] BELLE-II collaboration, *The Belle II Physics Book*, *PTEP* **2019** (2019) 123C01 [[1808.10567](#)].
- [72] FCC collaboration, *FCC-ee: The Lepton Collider: Future Circular Collider Conceptual Design Report Volume 2*, *Eur. Phys. J. ST* **228** (2019) 261.
- [73] G. Bernardi et al., *The Future Circular Collider: a Summary for the US 2021 Snowmass Process*, in *Snowmass 2021*, 3, 2022 [[2203.06520](#)].
- [74] CEPC STUDY GROUP collaboration, *CEPC Conceptual Design Report: Volume 2 - Physics & Detector*, [1811.10545](#).
- [75] CEPC PHYSICS STUDY GROUP collaboration, *The Physics potential of the CEPC. Prepared for the US Snowmass Community Planning Exercise (Snowmass 2021)*, in *Snowmass 2021*, 5, 2022 [[2205.08553](#)].
- [76] L. Li, M. Ruan, Y. Wang and Y. Wang, *Analysis of $B_s \rightarrow \phi\nu\bar{\nu}$ at CEPC*, *Phys. Rev. D* **105** (2022) 114036 [[2201.07374](#)].
- [77] Y. Amhis, M. Kenzie, M. Reboud and A.R. Wiederhold, *Prospects for searches of $b \rightarrow s\nu\bar{\nu}$ decays at FCC-ee*, *JHEP* **01** (2024) 144 [[2309.11353](#)].
- [78] T. Mannel and G.A. Schuler, *Semileptonic decays of bottom baryons at LEP*, *Phys. Lett. B* **279** (1992) 194.

- [79] A.F. Falk and M.E. Peskin, *Production, decay, and polarization of excited heavy hadrons*, *Phys. Rev. D* **49** (1994) 3320 [[hep-ph/9308241](#)].
- [80] ALEPH collaboration, *Measurement of Λ_b polarization in Z decays*, *Phys. Lett. B* **365** (1996) 437.
- [81] OPAL collaboration, *Measurement of the average polarization of b baryons in hadronic Z^0 decays*, *Phys. Lett. B* **444** (1998) 539 [[hep-ex/9808006](#)].
- [82] DELPHI collaboration, *Λ_b polarization in Z^0 decays at LEP*, *Phys. Lett. B* **474** (2000) 205.
- [83] C.-H. Chen and C.Q. Geng, *Study of $\Lambda_b \rightarrow \Lambda\nu\bar{\nu}$ with polarized baryons*, *Phys. Rev. D* **63** (2001) 054005 [[hep-ph/0012003](#)].
- [84] T.M. Aliev and M. Savci, *Unparticle physics effects in $\Lambda_b \rightarrow \Lambda+$ missing energy processes*, *Phys. Lett. B* **662** (2008) 165 [[0710.1505](#)].
- [85] B.B. Sirvanli, *Semileptonic $\Lambda_b \rightarrow \Lambda\nu\bar{\nu}$ decay in the Leptophobic Z -prime model*, *Mod. Phys. Lett. A* **23** (2008) 347 [[hep-ph/0701173](#)].
- [86] G. Hiller and R. Zwicky, *Endpoint relations for baryons*, *JHEP* **11** (2021) 073 [[2107.12993](#)].
- [87] N. Das and R. Dutta, *New physics analysis of $\Lambda_b \rightarrow (\Lambda^*(\rightarrow pK^-), \Lambda(\rightarrow p\pi))(\mu^+\mu^-, \nu\bar{\nu})$ baryonic decays under SMEFT framework*, *Phys. Rev. D* **108** (2023) 095051 [[2307.03615](#)].
- [88] G. Hiller and A. Kagan, *Probing for new physics in polarized Λ_b decays at the Z* , *Phys. Rev. D* **65** (2002) 074038 [[hep-ph/0108074](#)].
- [89] LHCb collaboration, *Differential branching fraction and angular analysis of $\Lambda_b^0 \rightarrow \Lambda\mu^+\mu^-$ decays*, *JHEP* **06** (2015) 115 [[1503.07138](#)].
- [90] LHCb collaboration, *Angular moments of the decay $\Lambda_b^0 \rightarrow \Lambda\mu^+\mu^-$ at low hadronic recoil*, *JHEP* **09** (2018) 146 [[1808.00264](#)].
- [91] W. Detmold, C.J.D. Lin, S. Meinel and M. Wingate, *$\Lambda_b \rightarrow \Lambda\ell^+\ell^-$ form factors and differential branching fraction from lattice QCD*, *Phys. Rev. D* **87** (2013) 074502 [[1212.4827](#)].
- [92] P. Böer, T. Feldmann and D. van Dyk, *Angular Analysis of the Decay $\Lambda_b \rightarrow \Lambda(\rightarrow N\pi)\ell^+\ell^-$* , *JHEP* **01** (2015) 155 [[1410.2115](#)].
- [93] L. Mott and W. Roberts, *Lepton polarization asymmetries for FCNC decays of the Λ_b baryon*, *Int. J. Mod. Phys. A* **30** (2015) 1550172 [[1506.04106](#)].
- [94] W. Detmold and S. Meinel, *$\Lambda_b \rightarrow \Lambda\ell^+\ell^-$ form factors, differential branching fraction, and angular observables from lattice QCD with relativistic b quarks*, *Phys. Rev. D* **93** (2016)

- 074501 [1602.01399].
- [95] T. Blake and M. Kreps, *Angular distribution of polarised Λ_b baryons decaying to $\Lambda\ell^+\ell^-$* , *JHEP* **11** (2017) 138 [1710.00746].
- [96] S. Roy, R. Sain and R. Sinha, *Lepton mass effects and angular observables in $\Lambda_b \rightarrow \Lambda(\rightarrow p\pi)\ell^+\ell^-$* , *Phys. Rev. D* **96** (2017) 116005 [1710.01335].
- [97] T. Blake, S. Meinel and D. van Dyk, *Bayesian Analysis of $b \rightarrow s\mu^+\mu^-$ Wilson Coefficients using the Full Angular Distribution of $\Lambda_b \rightarrow \Lambda(\rightarrow p\pi^-)\mu^+\mu^-$ Decays*, *Phys. Rev. D* **101** (2020) 035023 [1912.05811].
- [98] T. Blake, S. Meinel, M. Rahimi and D. van Dyk, *Dispersive bounds for local form factors in $\Lambda_b \rightarrow \Lambda$ transitions*, *Phys. Rev. D* **108** (2023) 094509 [2205.06041].
- [99] S. Meinel and G. Rendon, *$\Lambda_b \rightarrow \Lambda^*(1520)\ell^+\ell^-$ form factors from lattice QCD*, *Phys. Rev. D* **103** (2021) 074505 [2009.09313].
- [100] M. Bordone, *Heavy Quark Expansion of $\Lambda_b \rightarrow \Lambda^*(1520)$ Form Factors beyond Leading Order*, *Symmetry* **13** (2021) 531 [2101.12028].
- [101] S. Meinel and G. Rendon, *$\Lambda_c \rightarrow \Lambda^*(1520)$ form factors from lattice QCD and improved analysis of the $\Lambda_b \rightarrow \Lambda^*(1520)$ and $\Lambda_b \rightarrow \Lambda_c^*(2595, 2625)$ form factors*, *Phys. Rev. D* **105** (2022) 054511 [2107.13140].
- [102] Y. Amhis, M. Bordone and M. Reboud, *Dispersive analysis of $\Lambda_b \rightarrow \Lambda(1520)$ local form factors*, *JHEP* **02** (2023) 010 [2208.08937].
- [103] S. Descotes-Genon and M. Novoa-Brunet, *Angular analysis of the rare decay $\Lambda_b \rightarrow \Lambda(1520)(\rightarrow NK)\ell^+\ell^-$* , *JHEP* **06** (2019) 136 [1903.00448].
- [104] D. Das and J. Das, *The $\Lambda_b \rightarrow \Lambda^*(1520)(\rightarrow N\bar{K})\ell^+\ell^-$ decay at low-recoil in HQET*, *JHEP* **07** (2020) 002 [2003.08366].
- [105] Y. Amhis, S. Descotes-Genon, C. Marin Benito, M. Novoa-Brunet and M.-H. Schune, *Prospects for New Physics searches with $\Lambda_b^0 \rightarrow \Lambda(1520)\ell^+\ell^-$ decays*, *Eur. Phys. J. Plus* **136** (2021) 614 [2005.09602].
- [106] Y.-S. Li, S.-P. Jin, J. Gao and X. Liu, *Transition form factors and angular distributions of the $\Lambda_b \rightarrow \Lambda(1520)(\rightarrow NK)\ell^+\ell^-$ decay supported by baryon spectroscopy*, *Phys. Rev. D* **107** (2023) 093003 [2210.04640].
- [107] A. Beck, T. Blake and M. Kreps, *Angular distribution of $\Lambda_b^0 \rightarrow pK^-\ell^+\ell^-$ decays comprising Λ resonances with $spin \leq 5/2$* , *JHEP* **02** (2023) 189 [2210.09988].

- [108] LHCb collaboration, *Observation of the decay $\Lambda_b^0 \rightarrow pK^-\mu^+\mu^-$ and a search for CP violation*, *JHEP* **06** (2017) 108 [1703.00256].
- [109] LHCb collaboration, *Test of lepton universality with $\Lambda_b^0 \rightarrow pK^-\ell^+\ell^-$ decays*, *JHEP* **05** (2020) 040 [1912.08139].
- [110] LHCb collaboration, *Measurement of the $\Lambda_b^0 \rightarrow \Lambda(1520)\mu^+\mu^-$ Differential Branching Fraction*, *Phys. Rev. Lett.* **131** (2023) 151801 [2302.08262].
- [111] LHCb collaboration, *Analysis of $\Lambda_b^0 \rightarrow pK^-\mu^+\mu^-$ decays*, **2409.12629**.
- [112] J. Brod, M. Gorbahn and E. Stamou, *Two-Loop Electroweak Corrections for the $K \rightarrow \pi\nu\bar{\nu}$ Decays*, *Phys. Rev. D* **83** (2011) 034030 [1009.0947].
- [113] J. Brod, M. Gorbahn and E. Stamou, *Updated Standard Model Prediction for $K \rightarrow \pi\nu\bar{\nu}$ and ϵ_K* , *PoS BEAUTY2020* (2021) 056 [2105.02868].
- [114] PARTICLE DATA GROUP collaboration, *Review of Particle Physics*, *PTEP* **2022** (2022) 083C01.
- [115] F. Herren and M. Steinhauser, *Version 3 of RunDec and CRunDec*, *Comput. Phys. Commun.* **224** (2018) 333 [1703.03751].
- [116] T. Feldmann and M.W.Y. Yip, *Form factors for $\Lambda_b \rightarrow \Lambda$ transitions in the soft-collinear effective theory*, *Phys. Rev. D* **85** (2012) 014035 [1111.1844].
- [117] B. Mele and G. Altarelli, *Lepton spectra as a measure of b quark polarization at LEP*, *Phys. Lett. B* **299** (1993) 345.
- [118] G. Bonvicini and L. Randall, *Optimized variables for the study of Lambda(b) polarization*, *Phys. Rev. Lett.* **73** (1994) 392 [hep-ph/9401299].
- [119] C. Diaconu, M. Talby, J.G. Korner and D. Pirjol, *Improved variables for measuring the Λ_b polarization*, *Phys. Rev. D* **53** (1996) 6186 [hep-ph/9512330].
- [120] CMS collaboration, *Measurement of the Λ_b polarization and angular parameters in $\Lambda_b \rightarrow J/\psi\Lambda$ decays from pp collisions at $\sqrt{s} = 7$ and 8 TeV*, *Phys. Rev. D* **97** (2018) 072010 [1802.04867].
- [121] LHCb collaboration, *Measurement of the $\Lambda_b^0 \rightarrow J/\psi\Lambda$ angular distribution and the Λ_b^0 polarisation in pp collisions*, *JHEP* **06** (2020) 110 [2004.10563].
- [122] W. Altmannshofer, P. Stangl and D.M. Straub, *Interpreting Hints for Lepton Flavor Universality Violation*, *Phys. Rev. D* **96** (2017) 055008 [1704.05435].

- [123] L. Di Luzio and M. Nardecchia, *What is the scale of new physics behind the B-flavour anomalies?*, *Eur. Phys. J. C* **77** (2017) 536 [[1706.01868](#)].
- [124] SLD collaboration, *Measurement of the B hadron energy distribution in Z0 decays*, *Phys. Rev. D* **56** (1997) 5310 [[hep-ex/9707011](#)].